Pulse Radiolysis Investigation on the Mechanism of the Catalytic Action of Mn(II)−Pentaazamacrocycle Compounds as Superoxide Dismutase Mimetics

Andrej Maroz,[†] Geoffrey F. Kelso,[‡] Robin A. J. Smith,[§] David C. Ware,[†] and Robert F. Anderson*

Department of Chemistry, The University of Auckland, Private Bag 92019, Auckland 1142, New Zealand, Centre for Green Chemistry, Monash University, P.O. Box 75, Clayton, Victoria 3800, Australia, Department of Chemistry, University of Otago, Box 56, Dunedin 9054, New Zealand

Received: January 23, 2008; Revised Manuscript Received: February 28, 2008

The mechanism for the catalytic dismutation of superoxide by the Mn(II) pentaazamacrocyclic compound M40403 ([manganese(II) dichloro-(4*R*,9*R*,14*R*,19*R*)-3,10,13,20,26 pentaazatetracyclo [20.3.1.0^{4,9}.0^{14,9}] hexacosa-1(26),-22(23),24-triene], SODm1) and two 2,21-dimethyl analogues has been investigated using pulse radiolysis. The initial rate of reaction between superoxide and the manganese compounds was found to be dependent on structure and pH, with the resulting transient adducts possessing spectral characteristics of the metal center being oxidized to Mn(III). Values for the pK_a of the transient adducts (pK_a = 5.65 ± 0.05; 5.3 ± 0.1 and <5 for SODm1, SODm2 and SODm3, respectively) were obtained from spectrophotometric and conductivity measurements. Reaction of these transient adducts with further superoxide was highly structure dependent with the 2*S*,21*S*-dimethyl derivative (SODm2) being highly catalytically active at pH 7.4 (k_{cat} = 2.35 × 10^8 M^{-1} s^{-1}) compared to SODm1 (k_{cat} = 3.55 × 10^6 M^{-1} s^{-1}). In contrast the 2*R*,21*R*-dimethyl derivative (SODm3) showed no dismutation catalysis at all. The reaction rates of the initial complexes with $HO_2^•$ were significantly lower than with $O_2^{•-}$, and it is proposed that $O_2^{•-}$ is the main reactant in the catalytic cycle at pH 7.4. Variable temperature studies revealed major differences in the thermodynamics of the catalytic cycles involving SODm2 or SODm1. In the case of SODm2, the observed high entropic contribution to the activation energy is indicative of ligand conformational changes during the catalytic step. These results have provided the basis for a new mechanism for the catalytic dismutation of superoxide by Mn(II)−pentaazamacrocycle SOD mimetics.

Introduction

Mammalian cells are constantly exposed to the superoxide anion ($O_2^{•-}$), which mainly arises as a metabolic byproduct in the respiratory chain.[1] Under normal circumstances, the intracellular level of $O_2^{•-}$ is controlled by superoxide dismutases (SOD), a group of endogenous enzymes that catalyze the transformation of $O_2^{•-}$ into dioxygen and hydrogen peroxide.[2] However, during oxidative stress, such as in the case of acute or chronic inflammation, $O_2^{•-}$ production exceeds the level at which these enzymes can cope. In such cases, treatment with exogenous SOD to reinforce the natural defensive mechanisms has been tried. However, the use of exogenous SOD, such as that sourced as bovine SOD, is limited by both its size (M_r ∼ 30 kDa) and complexity, which affects cell permeability and causes immunological problems.[3–6] This has stimulated the search for synthetic, nonpeptidic compounds which can mimic the dismutating activity of the natural enzymes and are more readily bioavailable. Some of the lead compounds in this field of endeavor are based on Mn(III)−porphyrins with modified ligands[7–9] as well as Mn(III) salen complexes.[3,10] Several of the porphyrin SOD mimetics are reported to approach the catalytic activity of natural SOD (k_{cat} ∼ 10^9 M^{-1} s^{-1}), being active not only toward $O_2^{•-}$ but also with $CO_3^{•-}$, $ONOO^-$ and $NO^•$.[11] However, nonselective radical scavenging can be considered as a disadvantage, as reaction with other radicals can lead to the loss of SOD activity, as is known for natural MnSOD.[12,13] In the past decade, another approach to develop efficient SOD mimetics, based on Mn(II)−pentaazamacrocyclic complexes, has been particularly successful and an analogue has been produced which exhibits specific activity comparable to that of natural SOD.[3,14,15] The SOD activity of these complexes is strongly dependent on the ligand structure, and inversion of only one chiral center can result in a completely catalytically inactive compound.[16] Early attempts to study the mechanism by which these complexes dismutate superoxide have been carried out using the stopped-flow method.[17] However, this approach does not allow direct observation of intermediates nor a detailed study of the individual steps of the catalytic cycle. In this work we have utilized the faster time-resolution of pulse radiolysis to obtain a more comprehensive insight into the reactions of superoxide with these Mn(II)−pentaazamacrocyclic SOD mimetics.

Three different Mn(II)−pentaazamacrocycle complexes (SODm1−3) were studied (Scheme 1) with the objectives of determining the nature of the intermediates formed, the rate constants of the reaction of the compounds with superoxide and the catalytic SOD activities (k_{cat}). Our data enable a thermodynamic description to be made for the functioning of these complexes.

Materials and Methods

Materials. All chemicals were of analytical grade and were used as received. Water for preparation of the solutions was purified using a Milli-Q system. SODm1 was prepared as

* Corresponding author. Fax:(+64)9-3737422. E-mail: r.anderson@auckland.ac.nz.
[†] The University of Auckland. E-mail: A.M., a.maroz@auckland.ac.nz; D.C.W., d.ware@auckland.ac.nz.
[‡] Monash University. E-mail: Geoff.Kelso@sci.monash.edu.au.
[§] University of Otago. E-mail: rajsmith@chemistry.otago.ac.nz.

10.1021/jp800690u CCC: $40.75
Published on Web 05/13/2008

SCHEME 1: Structures of Mn(II)−Pentaazamacrocyclic SOD Mimetics Studied in This Work

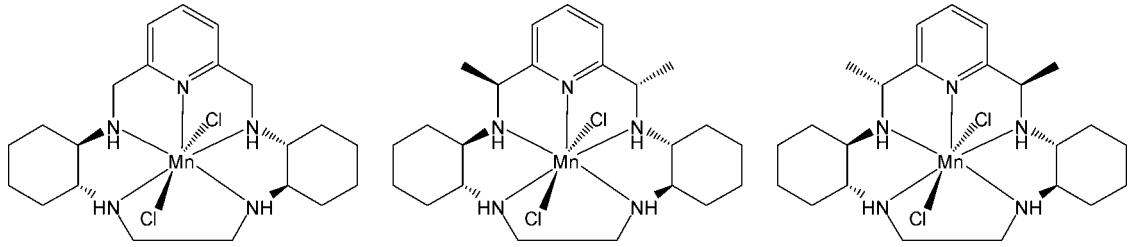

originally described[18] with further modifications.[19] SODm2 and SODm3 were prepared as reported.[15]

Pulse Radiolysis. Pulse radiolysis experiments were carried out using the University of Auckland's linear accelerator producing 4 MeV electron pulses of 200 ns to 1.5 μs duration, to deliver doses over the range 2−100 Gy. Data acquisition, dosimetry and radical detection systems have been previously described.[20] The pH of the solutions was controlled using phosphate buffers (10 mM) and adjusted to low and high pH using $HClO_4$ and NaOH, respectively, when required. Non-buffered solutions were used for conductivity studies and compared to N_2O-saturated solutions containing dimethylsulfoxide (1 mM) at low and high pH as the reference standard. Oxygenated solutions were bubbled with pure oxygen for 15 min. *tert*-Butanol (0.2 M) or sodium formate (25 mM) were used as $^{\bullet}OH$ radical scavengers. Experiments were routinely carried out at room temperature, 22 ± 2 °C.

Electrochemistry. Cyclic voltammetry was carried out under N_2 in dry acetonitrile solutions of the complexes (1 mM) containing $[(n\text{-}Bu)_4N](PF_6)$ (0.1 M) as the supporting electrolyte. A BAS 100A electrochemical workstation and standard three electrode cell was used. The BAS-supplied electrodes used were glassy carbon (working electrode), platinum wire (counter electrode) and Ag/Ag (3 M NaCl) (reference electrode). Ferrocene (Fc) was used as an internal standard.

Results

Reaction of Superoxide with SOD Mimetics. Superoxide was produced by the pulse radiolysis (2.5 Gy in 200 ns) of oxygen-saturated aqueous solutions containing sodium formate (25 mM) and phosphate buffers (10 mM). Under these conditions all of the primary radicals formed by the radiolysis of water (reaction 1, yield values in μM Gy^{-1} are given in parentheses) are converted into superoxide, $O_2^{\bullet-}$, reactions 25.

$$H_2O \rightarrow e^-_{aq}\ (0.28),\ ^{\bullet}OH\ (0.28),\ ^{\bullet}H\ (0.06),\ H_3O^+\ (0.28),\ H_2O_2\ (0.07),\ H_2\ (0.04) \quad (1)$$

$$e^-_{aq} + O_2 \rightarrow O_2^{\bullet-} \quad (2)$$

$$^{\bullet}H + O_2 \rightarrow HO_2^{\bullet} \quad (3)$$

$$^{\bullet}OH + HCO_2^- \rightarrow CO_2^{\bullet-} + H_2O \quad (4)$$

$$CO_2^{\bullet-} + O_2 \rightarrow CO_2 + O_2^{\bullet-} \quad (5)$$

Superoxide was found to react with the complexes to form transients which absorb in the UV−vis region.

$$O_2^{\bullet-} + [Mn^{II}(L)]^{2+} \rightarrow [Mn^{III}(L)O_2]^+ \quad (6)$$

The rate constants for reaction 6 were determined under pseudo-first-order conditions, where the concentration of the complexes was varied in great excess (20−100 μM) over the radiolytically produced $O_2^{\bullet-}$ (1.55 μM). The observed rate constants were plotted against the concentrations of the complexes to obtain second-order rate constants (Figure 1). The results show that $O_2^{\bullet-}$ reacts with SODm2 ($k_6 \approx 1.8 \times 10^9$ M^{-1} s^{-1}) about 20 times faster than with the other Mn(II)−pentaazamacrocyclic complexes under investigation ($k_6 \approx 9 \times 10^7$ M^{-1} s^{-1} for SODm1) (Table 1).

To determine the nature of the intermediate complex formed between $O_2^{\bullet-}$ and the investigated compounds, reaction 6, we first recorded the absorption spectrum of the transient formed upon the reaction of $O_2^{\bullet-}$ with SODm2. This spectrum has a characteristic band at 310 nm and was found to be different to that produced upon one-electron reduction of SODm2 by $CO_2^{\bullet-}$, which presumably reduces the Mn(II) to Mn(I) in a diffusion-controlled ($k_7 = 3.4 \times 10^9$ M^{-1} s^{-1}) process, reaction 7, to give rise to a transient which has a distinctive band centered at 415 nm, Figure 2.

$$CO_2^{\bullet-} + [Mn^{II}(L)]^{2+} \rightarrow CO_2 + [Mn^{I}(L)]^+ \quad (7)$$

The one-electron oxidation of SODm2 was carried out using the $SeO_3^{\bullet-}$ radical, which was produced by the scavenging of the e^-_{aq} by SeO_4^{2-}anions, and the $^{\bullet}OH/H^{\bullet}$ were scavenged by added *tert*-butanol to produce an inert radical.[21,22] Oxidation of Mn(II) to Mn(III) in the complex by the $SeO_3^{\bullet-}$ radical, has occurred rapidly with a rate constant of $k = 3.5 \times 10^9$ M^{-1} s^{-1}, reaction 8.

$$SeO_3^{\bullet-} + [Mn^{II}(L)]^{2+} \rightarrow SeO_3^{2-} + [Mn^{III}(L)]^{3+} \quad (8)$$

The absorption spectrum of the oxidized complex exhibits a rising band in the region below 370 nm, similar to that observed following the reaction of $O_2^{\bullet-}$ with the complex. The spectra

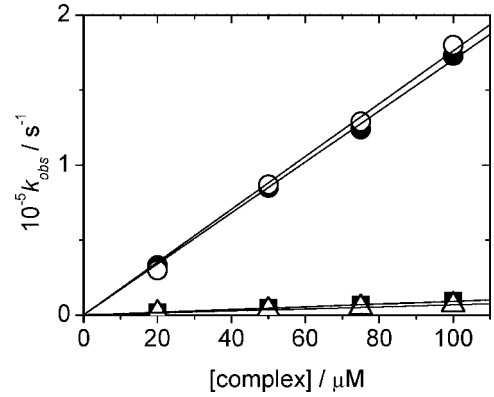

Figure 1. Observed first-order rate constants for the reaction of superoxide with increasing concentrations of SODm1 (squares), SODm2 (circles), SODm3 (triangles) at pH 7.4 (filled symbols) and pH 8.0 (open symbols). Kinetics measured for the absorption increase at 320 nm following the pulse radiolysis (2.5 Gy in 200 ns) of oxygen-saturated aqueous solutions of the complexes in the presence of sodium formate (25 mM) and phosphate buffer (10 mM).

TABLE 1: Rate Constants for the Reaction of Superoxide with the Complexes, k_6, and Catalytic Activity of SOD Mimetics, k_{cat}, at pH 7.4 and pH 8.0

complex	$10^{-6}k_6$/ M^{-1} s^{-1} pH 7.4	$10^{-6}k_6$/ M^{-1} s^{-1} pH 8.0	$10^{-6}k_{cat}$/ M^{-1} s^{-1} pH 7.4	$10^{-6}k_{cat}$/ M^{-1} s^{-1} pH 8.0
SODm1	89 ± 4	90 ± 5	3.55 ± 0.11	2.6 ± 0.1
SODm2	1680 ± 100	1800 ± 100	235 ± 20	178 ± 15
SODm3	68 ± 5	66 ± 5	no catalysis	no catalysis

produced upon the reaction of $O_2^{\bullet-}$ with the complex at pH 7.4 and 3.5 are radically different from the spectrum of the reduced form (Figure 2) and the slight difference in shape can be attributed to the protonation state, as these pHs are on the opposite sides of the estimated pK_a of the complex (Figure 3). Overall, the results presented in Figure 2 indicate that $O_2^{\bullet-}$ oxidizes the SODm2 to yield an intermediate complex containing a Mn(III) center, reaction 6. Similar results were obtained with the other two complexes over the same pH conditions.

Reaction of Superoxide with SOD Mimetics−pH Studies. The pH dependence of the reaction of superoxide with the complexes was studied over the range 3.5−9.0. Transient absorption changes, observed at 320 nm (Figure 3), indicate that the intermediate complex, formed as per reaction 6, exists in both deprotonated and protonated forms (equilibrium 9):

$$[Mn^{III}(L)O_2]^+ + H^+ \rightleftharpoons [Mn^{III}(L)OOH]^{2+} \qquad (9)$$

The pK_a values of the intermediate complexes, determined from the changes in absorption (Figure 3), are 5.65 ± 0.05 (SODm1), 5.3 ± 0.1 (SODm2) and <5 (SODm3). Due to the method limitations it is not possible to estimate the pK_a for SODm3 with greater precision, as the absorption changes occur over wider pH range, resulting in larger error in a sigmoidal line fit of the experimental data.

The dependence of the second-order rate constants (k_6) on pH for the reaction of superoxide with the complexes is presented in Figure 4. The reaction rate constants decrease significantly when the pH is lower than the pK_a (4.8[23]) of the superoxide radical. This is probably due to a reduced reactivity of the complexes with the protonated form ($HO_2^{\bullet}$) of superoxide.

Conductivity Measurements. Changes in conductivity following the pulse radiolysis of solutions containing the complexes were compared to that of solutions containing dimethyl sulfoxide (DMSO) as a standard under N_2O saturated conditions. The sulfinic acid (pK_a = 2.28), which is formed upon irradiation of an aqueous solution of DMSO, results in known changes in conductivity under acidic and basic conditions.[24] When aqueous oxygenated solutions of SODm1 and SODm2 were irradiated at pH 4, a rapid increase in conductance followed by a decrease to near prepulse levels was observed (Figure 5). This observation is indicative of an inner sphere mechanism, where the superoxide enters the coordination sphere to bind to the metal center to give a transient intermediate which is protonated at pH 4 and hence has the same charge as the starting complex. At pH 10, immediately after the pulse, the conductivity decreased followed by a further smaller decrease (Figure 5). This is explained as an initial rapid neutralization of the protons (formed by the radiation pulse) by the hydroxide ions in solution and the decrease in conductivity of the transient intermediate formed in reaction 6 due to the reduced charge relative to the starting complex. The further decrease in conductivity at pH 10, observed at the millisecond time scale is attributed to the slow protonation of the complex.

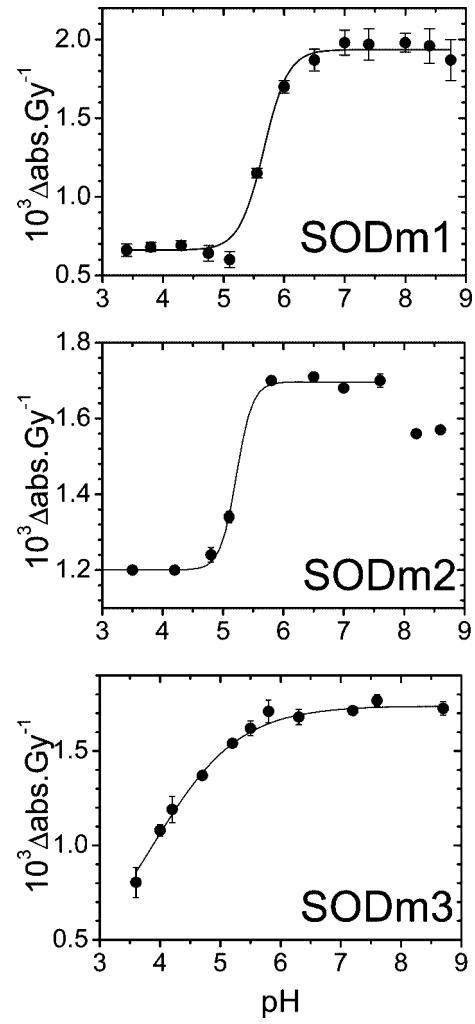

Figure 3. Dependence of the change in transient absorbance at 320 nm on pH following the pulse radiolysis (2.5 Gy in 200 ns) of oxygen-saturated aqueous solutions containing the complexes (0.1 mM), sodium formate (25 mM) and phosphate buffer (10 mM). The pK_a values for SODm1 and SODm2 intermediates of 5.65 ± 0.05 and 5.3 ± 0.1, respectively, are derived from sigmoidal fits, whereas the pK_a for SODm3 is estimated at <5.

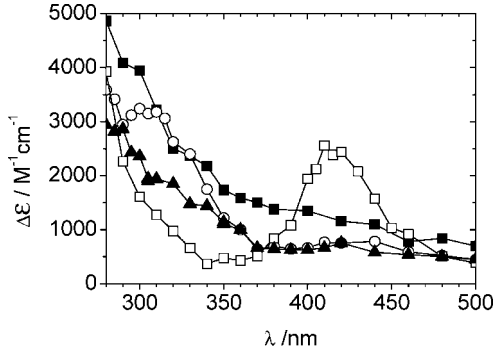

Figure 2. Absorption spectra observed at ca. 20 μs following the pulse radiolysis (2.5 Gy in 200 ns) of aqueous solutions of SODm2 (0.1 mM) containing phosphate buffer (10 mM) and (a) sodium formate (25 mM), pH 7.4, oxygen saturated (○); (b) sodium formate (25 mM), pH 3.5, oxygen saturated (▲); (c) sodium formate (25 mM), pH 7.4, deaerated (□); and (d) sodium selenate (25 mM), *tert*-butanol (0.2 M), pH 7.4, deaerated (■).

Catalytic Activity of SOD Mimetics. The rate constants for the catalytic removal of $O_2^{\bullet-}$, k_{cat}, were determined from the measured half-lives of $O_2^{\bullet-}$ in the absence and increasing concen-

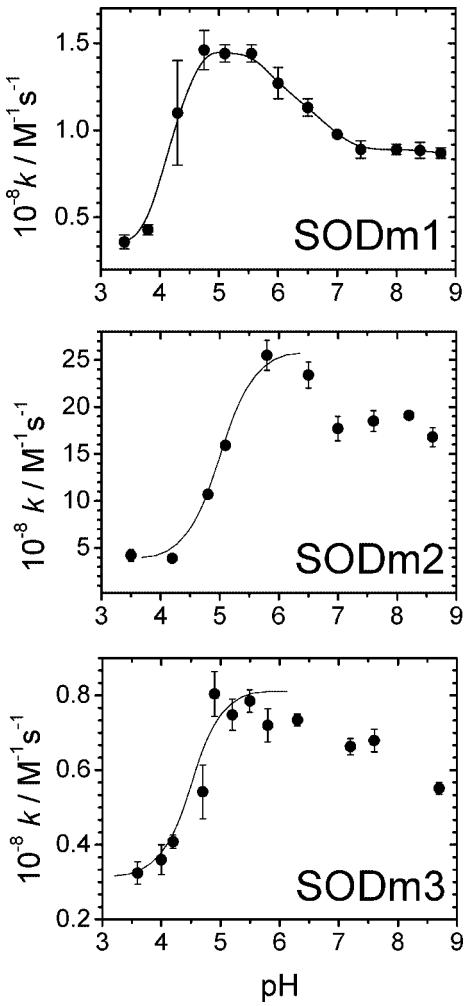

Figure 4. Dependence of the second-order rate constants for the reaction of superoxide with the complexes on pH. Experimental conditions are as in Figure 1. The reaction rate constants decrease significantly when the pH is lower than the pK_a (4.8[23]) of the superoxide radical, because of a reduced reactivity of the complexes with the protonated form ($HO_2^\bullet$) of superoxide.

trations of SODm1 (Figure 6) and SODm2 (Figure 7). To separate pseudo-first-order decay of $O_2^{\bullet-}$ by reaction with SOD complexes from second-order decay of $O_2^{\bullet-}$ by reaction with itself, the inverse in half-life of $O_2^{\bullet-}$ was plotted against the concentration of $O_2^{\bullet-}$ (Figure 6a). The intercepts give inverse half-lives for the pseudo-first-order decay of $O_2^{\bullet-}$in reaction with SOD complexes.[25] The rate constants derived from these half-lives were plotted against concentration of the SOD complex (Figure 6b). The slope of the fitted line provides the value for k_{cat}. Assuming a two-step scheme, viz. oxidation of the $[Mn^{II}(L)]^{2+}$ by $O_2^{\bullet-}$ to form the transient $[Mn^{III}(L)O_2]^+$ intermediate (k_6, reaction 6) followed by reaction with a second $O_2^{\bullet-}$ to reform the original $[Mn^{II}(L)]^{2+}$ together with O_2 and H_2O_2, k_{10}:

$$[Mn^{III}(L)O_2]^+ + O_2^{\bullet-} + 2H^+ \rightarrow [Mn^{II}(L)]^{2+} + O_2 + H_2O_2 \quad (10)$$

the dismutation rate can be described with the following equation:

$$-d[O_2^{\bullet-}]/dt = (2k_6k_{10}/(k_6 + k_{10}))[[Mn^{II}(L)]^{2+}][O_2^{\bullet-}] = k_{cat}[[Mn^{II}(L)]^{2+}][O_2^{\bullet-}]$$

Both SODm1 and SODm2 showed significant catalytic activity, even at micromolar concentrations, whereas SODm3 did not influence the decay of superoxide at both pH 7.4 and 8.0 when added in concentrations up to 50 μM (Table 1).

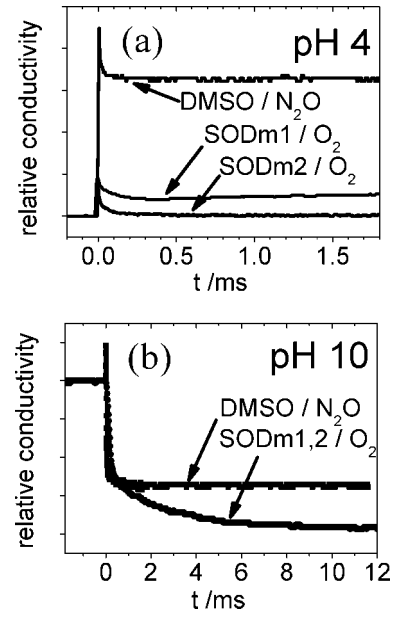

Figure 5. Kinetic traces, showing changes in conductivity following the pulse radiolysis (3 Gy in 200 ns) of oxygen-saturated aqueous solutions of the complexes (0.1 mM) containing *tert*-butanol (0.2 M) at (a) pH 4 and (b) pH 10. Conductivity changes are compared to that observed following the pulse radiolysis of N_2O-saturated aqueous solutions containing dimethylsulfoxide (1 mM) under the same conditions.

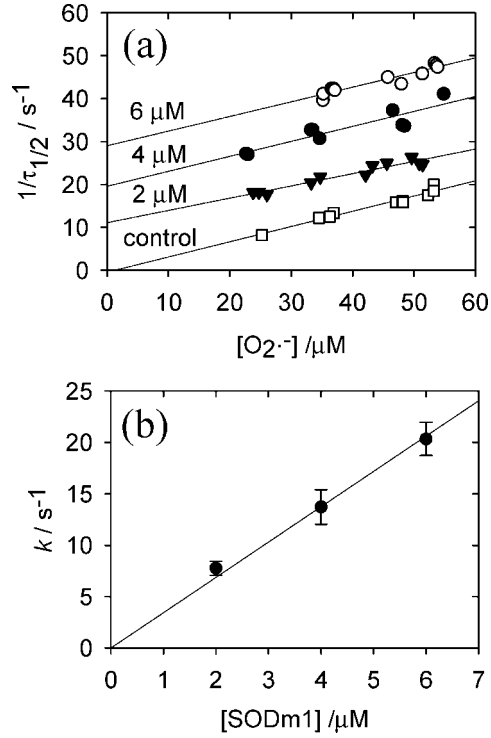

Figure 6. (a) Kinetic plots of the dependence of the inverse in half-life of superoxide, measured at 270 nm in the absence and with increasing concentrations of SODm1 at pH 7.4. (b) Dependence of rate constants for the reaction of SODm1 with superoxide (derived from intercepts of (a)) on the concentration of SODm1. The slope of the fitted line (b) provides the value for k_{cat} (Table 1). Data obtained in the pulse radiolysis (0−100 Gy in 1.5 μs) of oxygen-saturated aqueous solutions containing SODm1, sodium formate (25 mM) and phosphate buffer (10 mM) pH 7.4.

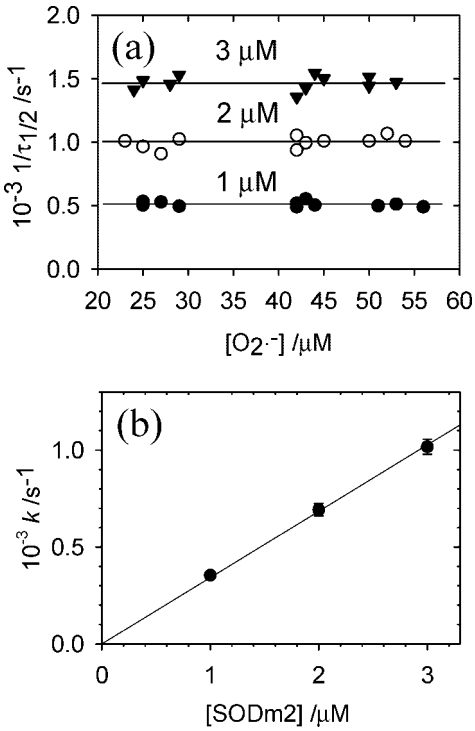

Figure 7. (a) Kinetic plots of the dependence of the inverse in half-life of superoxide in the presence of increasing concentrations of SODm2 at pH 7.4. (b) Dependence of rate constants for the reaction of superoxide with SODm2 (derived from intercepts of (a)) on the concentration of SODm2. The slope of the fitted line provides the value for k_{cat}. Experimental conditions are as in Figure 6.

Thermodynamics of the Catalytic Process. The reaction of $O_2^{\bullet-}$ with SODm1 and SODm2, as well as the catalytic activity of these complexes, were studied over the temperature range 15−45 °C (Figure 8). Eyring plots of k_6 for both SODm1 and SODm2 are very similar with the rate constants increasing with temperature. However for k_{cat}, which is the rate constant for the overall catalytic process, a different temperature dependence was observed for SODm1 and SODm2. The k_{cat} values for SODm2 exhibit an apparent decrease with temperature and this behavior is reflected in the thermodynamic parameters, presented in Table 2.

Redox Properties of Initial Mn^{II} Complexes. To determine the redox properties of the metal center in the complexes, quasi-reversible cyclic voltammetry measurements were carried out under N_2 using acetonitrile as the solvent (Figure 9). Ferrocene (Fc) was used as an internal standard so that the half-wave potential of the complexes could be directly compared to the half-wave potential of the Fc^+/Fc couple. The final redox potential values vs NHE were obtained using the known value for the ferrocene couple in acetonitrile ($E°$(Fc^+/Fc) vs SCE = 425 mV[26]), and the relation between the two reference electrodes: SCE vs NHE = 242 mV.[27] The measured redox potentials $E_{1/2}$(SODm Mn^{3+}/Mn^{2+}) were found to be 525, 464 and 452 mV for SODm1, SODm2 and SODm3, respectively. Given the similarity between the values obtained for the active (SODm2) and inactive (SODm3) catalysts, it is concluded that metal center oxidation is not a crucial (rate-determining) step in the catalytic process.

Discussion

The present study has relevance to the mechanism of catalytic action of Mn(II)−pentaazamacrocyclic compounds as superoxide dismutase mimetics (Scheme 1) at physiological pH. The pH values of 7.4 and 8.0 are typical for intracellular and intramitochondrial environments, respectively, where natural SOD activity is operative. Our data support the proposal, that at pH > 7.4 the catalytic cycle proceeds through the inner sphere mechanism. Introduction of the $O_2^{\bullet-}$ into the coordination sphere of the metal center is accompanied by the formation of Mn(III); i.e., metal center oxidation occurs. The directly observed intermediate complex, described as $[Mn^{III}(L)O_2]^+$, has a pK_a < 6, which is supported by both optical and conductivity measurements. Thus, at natural pH levels the intermediate exists predominantly in a deprotonated state.

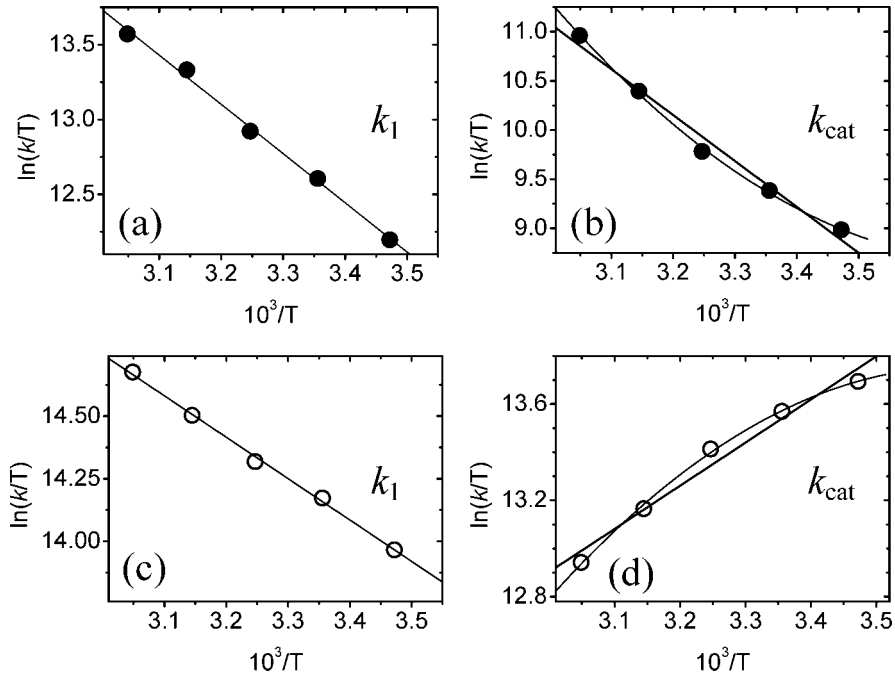

Figure 8. (a, c) Eyring plots for the reaction of superoxide with SODm1 (●) and SODm2 (○) over the temperature range 15 −45 °C. The rate constants, k_1, were determined as described in Figure 1. (b, d) Eyring plots for overall catalytic process. The rate constants, k_{cat}, were determined as described in Figures 6 and 7.

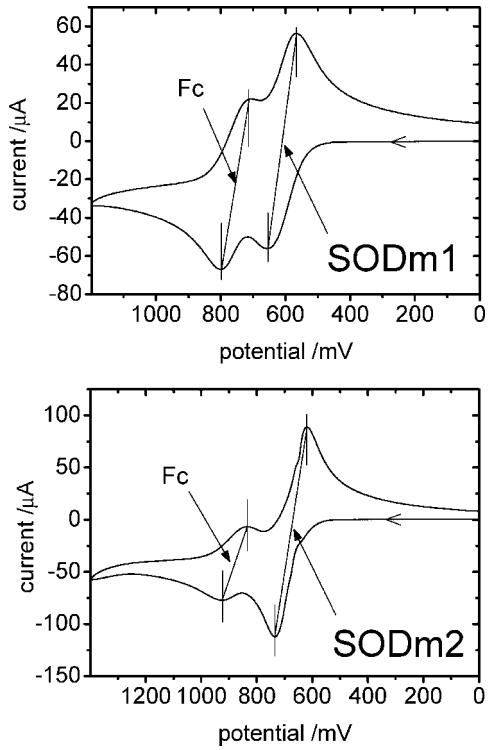

Figure 9. Examples of cyclic voltammetry measurements in acetonitrile for SODm1 and SODm2. Solutions contained the complexes (1 mM), $[(n\text{-Bu})_4N](PF_6)$ (0.1 M) as the supporting electrolyte and ferrocene (ca. 1 mM) as an internal standard, to determine the potential vs NHE. Measurements were taken with a scan rate of 50 mV/s. Redox potentials (vs NHE) are calculated to be $E_{1/2}$(SODm1 $[Mn^{3+}/Mn^{2+}]$) = 525 mV; $E_{1/2}$(SODm2 $[Mn^{3+}/Mn^{2+}]$) = 464 mV; $E_{1/2}$(SODm3 $[Mn^{3+}/Mn^{2+}]$) = 452 mV.

The mechanism by which Mn(II)−pentaazamacrocyclic compounds act as SOD mimetics, is very different from that of the native enzyme. Early pulse radiolysis studies show that the active center of native MnSOD contains Mn(III). The reduction of the metal center by $O_2^{\bullet-}$ is believed to occur as the first step of catalysis, immediately converting one equivalent of superoxide to oxygen without the formation of a complex. This was determined by indirect observation of the superoxide decay and loss of Mn(III) band at 480 nm.[28]

It has been stated in earlier studies that the SOD catalytic rate of Mn(II)−pentaazamacrocyclic compounds is governed by the rate of oxidation of the metal center, as being the rate-determining step in the mechanism.[29,30] However, our results indicate that the oxidation of the metal center is not the rate-determining step, as the moderately active catalyst, SODm1, reacts with $O_2^{\bullet-}$ at a rate similar to that of the ineffective catalyst, SODm3. An alternative mechanism, which has been proposed recently,[31] suggests a rate-determining role for the $Cl^- \leftrightarrow H_2O$ ligand exchange in the complexes. However, recent studies on the ligand exchange mechanism with seven-coordinate Mn(II) compounds question the potential rate-determining role of this process.[32] Moreover, our cyclic voltammetry measurements clearly demonstrate that the redox potential of the Mn(III)/Mn(II) couple is similar for two complexes with vastly differing SOD activities. It is clear from our work that the reaction of the initial Mn(II) compound with $O_2^{\bullet-}$ is an important step, as it produces the $[Mn^{III}(L)O_2]^+$, but it does not determine the overall catalytic rate. Furthermore, we suggest that the $[Mn^{III}(L)O_2]^+$ intermediate oxidizes the next molecule of $O_2^{\bullet-}$, and this process is a crucial point in the catalytic cycle.

Investigation of the conformational and coordinational changes of Mn−pentaazamacrocyclic complexes, using computational methods, has revealed differences in the geometry of Mn(II)−(pentagonal bipyramidal) and Mn(III)−(pseudooctahedral) compounds.[33] These data, obtained using a molecular mechanics method, which necessarily incorporates substantial approximations, were compared to solid state crystallography data that may not truly reflect the conformation of the ligand in the aqueous environment. Nonetheless, this approach was very useful for identifying structural features that enhance SOD activity and, in particular, indicated that flexibility in the ligand geometry could be a significant factor in the reaction. We propose, that the ability of a ligand to accommodate Mn(III) pseudo-octahedral coordination affects the second step of catalytic process and not the initial metal center oxidation as previously suggested.[15] This aspect is fully supported, and indeed enhanced, by our results (Table 2), which show the major influence of an entropy factor on the second stage of the catalytic process for the most effective (SODm2) catalyst. On the basis of the data obtained, we propose the following reaction mechanism (Scheme 2):

SCHEME 2: Proposed Catalytic Cycle

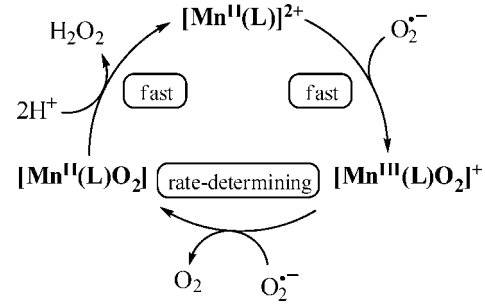

The overall mechanism consists of three steps:

1. Activation of the complex by reaction with $O_2^{\bullet-}$ (fast):

$$O_2^{\bullet-} + [Mn^{II}(L)]^{2+} \rightarrow [Mn^{III}(L)O_2]^+$$

The resulting intermediate Mn(III) complex is present in its deprotonated form at pH 7 and above ($pK_a \approx 5.5$, Figures 3 and 4).

2. Reduction of the activated intermediate complex by a further $O_2^{\bullet-}$, which is influenced greatly by its 3-dimensional structure. The metal center is reduced back to the initial Mn(II), although the intermediate pseudoctahedral geometry is maintained:

TABLE 2: Thermodynamic Properties for the Reactions of Superoxide with the Complexes at pH 7.4, Derived from Eyring Plots Presented in Figure 8

	k_6, $O_2^{\bullet-}$ + SODm1	k_{cat}, catalytic $O_2^{\bullet-}$ dismutation by SODm1	k_6, $O_2^{\bullet-}$ + SODm2	k_{cat}, catalytic $O_2^{\bullet-}$ dismutation by SODm2
ΔH^θ/kJ mol^{-1}	27.4	38.8	13.7	−14.9
ΔS^θ/J mol^{-1} K^{-1}	−1	11	−34	−135
$\Delta G_{298}{}^\theta$/kJ mol^{-1}	27.6	35.5	23.8	25.3

$$[Mn^{III}(L)O_2]^+ + O_2^{\bullet -} \rightarrow [Mn^{II}(L)O_2] + O_2$$

3. Proton-assisted release of the H_2O_2 with concomitant conformational relaxation of the Mn(II) complex to yield the starting compound with pentagonal-bipyramidal coordination sphere:

$$[Mn^{II}(L)O_2] + 2H^+ \rightarrow [Mn^{II}(L)]^{2+} + H_2O_2$$

This mechanism supports the view that the catalytic activity of the Mn(II)−pentaazamacrocyclic complexes is governed by the intermediate geometry of the $[Mn^{III}(L)O_2]^+$ and its reactivity with the second approaching $O_2^{\bullet -}$. In regard to the folding ability (pentagonal bipyramidal → pseudooctahedral) as previously proposed,[15] this ligand modification strategy is still viable, but structural modifications to the initial Mn(II) complexes should be dictated by the desirable structure of $[Mn^{III}(L)O_2]^+$ intermediate. As the catalytic activity of the natural enzyme ($k_{cat} \sim 10^9$ M^{-1} s^{-1}) is still unmatched by the existing SOD mimetics at physiological pH, there is scope for improvement to be made, possibly by changing the charge distribution in the ligand and substituent groups to increase its affinity for $O_2^{\bullet -}$.

Acknowledgment. This work is supported by grant UOA 0407 of the Marsden Fund from the Royal Society of New Zealand.

References and Notes

(1) Halliwell, B.; Gutteridge, J. M. C. *Free Radicals in Biology and Medicine*; Oxford University Press: New York, 1999.
(2) McCord, J. M. *Science* **1974**, *185*, 529.
(3) Salvemini, D.; Riley, D. P.; Cuzzocrea, S. *Nature Rev. Drug Discovery* **2002**, *1*, 367.
(4) Imaizumi, S.; Woolworth, V.; Fishman, R. A.; Chan, P. H. *Stroke* **1990**, *21*, 1312.
(5) Tagaya, M.; Matsumoto, M.; Kitagawa, K.; Niinobe, M.; Ohtsuki, T.; Hata, R.; Ogawa, S.; Handa, N.; Mikoshiba, K.; Kamada, T. *Life Sci.* **1992**, *51*, 253.
(6) Armstead, W. M.; Mirro, R.; Thelin, O. P.; Shibata, M.; Zuckerman, S. L.; Shanklin, D. R.; Busija, D. W.; Leffler, C. W. *Stroke* **1992**, *23*, 755.
(7) Batinić-Haberle, I.; Spasojević, I.; Stevens, R. D.; Hambright, P.; Fridovich, I. *J. Chem. Soc., Dalton Trans.* **2002**, 2689.
(8) Batinić-Haberle, I.; Spasojević, I.; Stevens, R. D.; Hambright, P.; Neta, P.; Okada-Matsumoto, A.; Fridovich, I. *Dalton Trans.* **2004**, 1696.
(9) Batinić-Haberle, I.; Spasojević, I.; Stevens, R. D.; Bondurant, B.; Okado-Matsumoto, A.; Fridovich, I.; Vujašković, Z.; Dewhirst, M. W. *Dalton Trans.* **2006**, 617.
(10) Gonzalez, P. K.; Zhuang, J.; Doctrow, S. R.; Malfroy, B.; Benson, P. F.; Menconi, M. J.; Fink, M. P. *J. Pharmacol. Exp. Ther.* **1995**, *275*, 798.
(11) Spasojević, I.; Batinić-Haberle, I.; Stevens, R. D.; Hambright, P.; Thorpe, A. N.; Grodkowski, J.; Neta, P.; Fridovich, I. *Inorg. Chem.* **2001**, *40*, 726.
(12) Muscoli, C.; Cuzzocrea, S.; Riley, D. P.; Zweier, J. L.; Thiemermann, C.; Wang, Z. Q.; Salvemini, D. *Br. J. Pharmacol.* **2003**, *140*, 445.
(13) MacMillan-Crow, L. A.; Crow, J. P.; Thompson, J. A. *Biochemistry* **1998**, *37*, 1613.
(14) Riley, D. P.; Henke, S. L.; Lennon, P. J.; Weiss, R. H.; Neumann, W. L.; Rivers, W. J.; Aston, K. W.; Sample, K. R.; Rahman, H.; Ling, C. S.; Shieh, J. J.; Busch, D. H.; Szulbinski, W. *Inorg. Chem.* **1996**, *35*, 5213.
(15) Aston, K.; Rath, N.; Naik, A.; Slomczynska, U.; Schall, O. F.; Riley, D. P. *Inorg. Chem.* **2001**, *40*, 1779.
(16) Riley, D. P.; Lennon, P. J.; Neumann, W. L.; Weiss, R. H. *J. Am. Chem. Soc.* **1997**, *119*, 6522.
(17) Riley, D. P.; Rivers, W. J.; Weiss, R. H. *Anal. Biochem.* **1991**, *196*, 344.
(18) Salvemini, D.; Wang, Z. Q.; Zweier, J. L.; Samouilov, A.; Macarthur, H.; Misko, T. P.; Currie, M. G.; Cuzzocrea, S.; Sikorski, J. A.; Riley, D. P. *Science* **1999**, *286*, 304.
(19) Riley, D. P.; Neumann, W. L.; Henke, S. L.; Lennon, P.; Aston, K. W.; Salvemini, D.; Sikorski, J. A.; Fobian, Y. M.; Grapperhaus, M. L.; Kusturin, C. L. Substituted pyridino pentaazamacrocycle complexes having superoxide dismutase activity as therapeutic agents; (Monsanto Company, USA). US Patent 6214187, 2001.
(20) Anderson, R. F.; Denny, W. A.; Li, W. J.; Packer, J. E.; Tercel, M.; Wilson, W. R. *J. Phys. Chem. A* **1997**, *101*, 9704.
(21) Neta, P.; Huie, R. E.; Ross, A. B. *J. Phys. Chem. Ref. Data* **1988**, *17*, 1027.
(22) Klaning, U. K.; Sehested, K. *J. Phys. Chem.* **1986**, *90*, 5460.
(23) Bielski, B. H. J.; Allen, A. O. *J. Phys. Chem.* **1977**, *81*, 1048.
(24) Asmus, K.-D.; Janata, E. Conductivity monitoring techniques. In *The study of fast processes and transient species by electron pulse radiolysis*; Baxendale, J. H., Busi, F., Ed.; Reidel: Dordrecht, 1982; pp 91.
(25) Anderson, R. F.; Shinde, S. S.; Hay, M. P.; Gamage, S. A.; Denny, W. A. *J. Am. Chem. Soc.* **2003**, *125*, 748.
(26) Gennett, T.; Milner, D. F.; Weaver, M. J. *J. Phys. Chem.* **1985**, *89*, 2787.
(27) Meites, L. *Handbook of Analytical Chemistry*; McGraw Hill: New York, 1963.
(28) McAdam, M. E.; Fox, R. A.; Lavelle, F.; Fielden, E. M. *Biochem. J.* **1977**, *165*, 71.
(29) Riley, D. P.; Weiss, R. H. *J. Am. Chem. Soc.* **1994**, *116*, 387.
(30) Riley, D. P. *Chem. Rev.* **1999**, *99*, 2573.
(31) Riley, D. P.; Schall, O. F. Structure-activity studies and the design of synthetic superoxide dismutase (SOD) mimetics as therapeutics. In *Advances in Inorganic Chemistry: Including Bioinorganic Studies*; Elsevier: Amsterdam, 2007; Vol. 59, pp 233.
(32) Dees, A.; Zahl, A.; Puchta, R.; Hommes, N.; Heinemann, F. W.; Ivanovic-Burmazovic, I. *Inorg. Chem.* **2007**, *46*, 2459.
(33) Riley, D. P.; Henke, S. L.; Lennon, P. J.; Aston, K. *Inorg. Chem.* **1999**, *38*, 1908.

JP800690U